Accelerator and Reactor Neutrino Experiments

Luigi DiLella
CERN
Geneva, Switzerland

1 Introduction

Since the first detection of the neutrino at reactors [1] and the discovery of the ν_μ at the Brookhaven AGS [2], accelerators and reactors have been used to provide intense beams of neutrinos. Over the last 30 years, experiments with neutrino beams have played a major role in shaping the Standard Model of particle physics as it is known today.

At present, electroweak theory is more conveniently studied at high energy hadron and electron colliders where the W and Z bosons are directly produced and their properties can be studied in great detail. Nevertheless, experiments with neutrino beams continue to play a major role in particle physics by addressing other crucial questions: are neutrinos massive? do they mix?

The search for neutrino oscillations is presently the most promising method to search for very small neutrino masses. The hypothesis of neutrino mixing postulates that the three known neutrino flavors, ν_e, ν_μ, and ν_τ, are not mass eigenstates but quantum-mechanical superpositions of three mass eigenstates, ν_1, ν_2, and ν_3, with mass eigenvalues m_1, m_2, and m_3, respectively:

$$\nu_\alpha = \sum_k U_{\alpha k}\ \nu_k\ . \tag{1}$$

In Eq. (1), $\alpha = e, \mu, \tau$ is the flavor index, $k = 1, 2, 3$ is the index of the mass eigenstates and U is a unitary 3×3 matrix. If mixing of two neutrinos is dominant, the probability to detect ν_β if the neutrino state at production is pure ν_α can be written as

$$P_{\alpha\beta}(L) = \sin^2(2\theta)\ \sin^2\left(1.27\ \Delta m^2\ \frac{L}{E}\right) \tag{2}$$

where θ is the mixing angle, L is the distance between the neutrino source and the detector in km, $\Delta m^2 = |m_1^2 - m_2^2|$ is in eV^2 and E is in GeV. Depending on L and E, experiments are sensitive to different Δm^2 regions.

2 Neutrino oscillation searches at nuclear reactors

Nuclear reactors are intense, isotropic sources of $\overline{\nu}_e$ produced by β-decay of fission fragments. The $\overline{\nu}_e$ energy is below 10 MeV, with an average value of ~ 3 MeV. Their energy spectrum and flux above 2 MeV have been measured [3]. From the knowledge of the reactor parameters, the $\overline{\nu}_e$ flux is predicted with an uncertainty of 2.7%.

The inverse β-decay reaction

$$\overline{\nu}_e + p \rightarrow e^+ + n \tag{3}$$

is used to detect reactor neutrinos. This reaction has a threshold of 1.8 MeV and gives rise to two detectable signals: a prompt one from e^+ production and annihilation into two photons; and a late photon signal from neutron capture (2.2 MeV from the reaction $np \rightarrow d\gamma$, ~ 8 MeV from neutron capture by Gadolinium in Gd-doped scintillator).

Table 1 lists the main parameters of the two long baseline experiments which have recently reported results.

The Chooz experiment is named after the site of a nuclear power plant (the village of Chooz in the Ardennes region of France). The measured positron spectrum agrees with the spectrum expected in the absence of neutrino oscillations, as shown in Fig. 1. The energy-integrated ratio between the measured and expected event rate is found to be [4]

$$R = 1.010 \pm 0.028 \text{ (stat.)} \pm 0.027 \text{ (syst.)} \tag{4}$$

	Chooz [4]	Palo Verde [5]
Number of reactors	2	3
Distance (Km)	1.114, 0.998	0.89, 0.89, 0.75
Thermal power (GW)	8.5	11.0
Detector type	Gd-doped homogeneous scintillator	Gd-doped segmented scintillator
Detector mass	5 Tons	12 Tons
Rock overburden	300 m w.e.	32 m w.e.
Event rate (at full power)	25.5 ± 1.0 d^{-1}	39.1 ± 1.0 d^{-1}
Event rate (reactors off)	1.1 ± 0.3 d^{-1}	32.6 ± 1.0 d^{-1}
Status	Completed	In progress

Table 1: Long baseline reactor experiments.

Figure 2 shows the region of $\overline{\nu}_e - \overline{\nu}_x$ oscillation parameters excluded at the 90% confidence level. This result strongly constrains the contribution from a possible $\nu_\mu - \nu_e$ oscillation to the deficit of atmospheric ν_μ observed by many experiments [6].

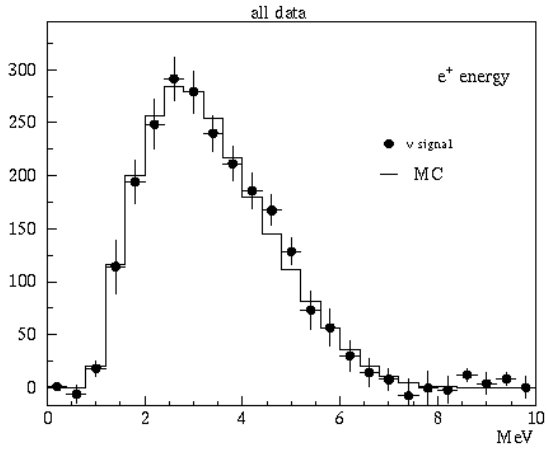

Figure 1: Expected positron spectrum for the case of no oscillation (histogram), superimposed on the measured spectrum in the Chooz experiment [4].

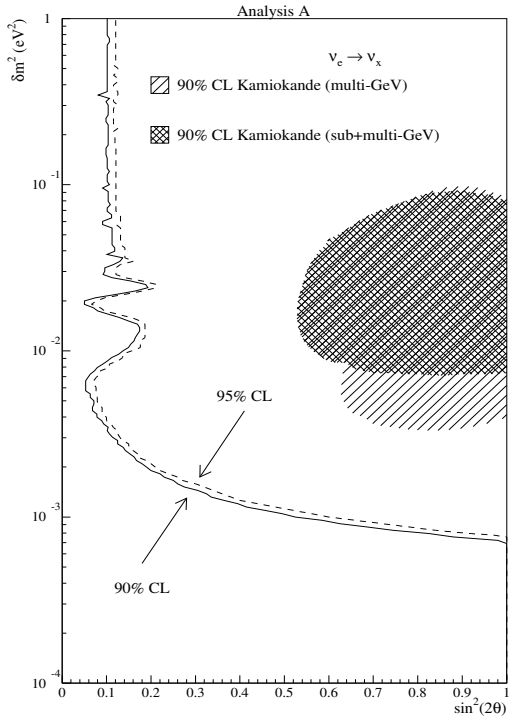

Figure 2: Boundary of the $\overline{\nu}_e - \overline{\nu}_x$ oscillation parameter region excluded by the comparison of the measured positron spectrum with the spectrum expected in the absence of $\overline{\nu}_e$ allowed by the results of Ref. [7].

An analysis of the Chooz data that does not rely on the absolute knowledge of the $\overline{\nu}_e$ flux has also been performed by taking advantage of the fact that a substantial amount of data was taken with only one reactor in operation. The comparison of the measured positron spectra from each reactor provides a direct determination of the oscillation probability because, as shown in Table 1, the two reactors are at different distances. The region of oscillation parameters excluded by this analysis [4] is shown in Fig. 3.

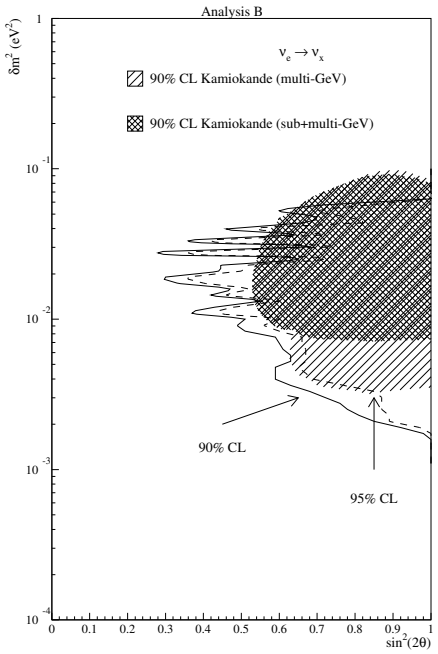

Figure 3: Exclusion contours at 90% and 95% confidence level obtained from the ratio of the positron spectra from the two reactors, as measured by the Chooz experiment. Also shown is the region of $\nu_\mu - \nu_e$ oscillation parameters allowed by the results of Ref. [7].

In the Palo Verde experiment [5], because of the shallow site, the background is much higher than in the Chooz experiment (see Table 1). From the data collected in 1998 during the first 70 day run, this experiment has reported the value

$$R = 1.3 \pm 0.3 \text{ (stat.)} \pm 0.2 \text{ (syst.)}$$

for the ratio between the measured event rate and the rate expected in the absence of $\overline{\nu}_e$ oscillations. This result is much less sensitive to oscillations than the final result from the Chooz experiment (see Eq. 4).

3 Future oscillation searches at reactors

KAMLAND [8] is a long baseline reactor experiment which will begin data taking in 2001. The detector consists of $\sim$ 1000 tons of scintillating isoparaffin oil, installed in the Kamioka mine at a depth of 2700 m of water equivalent.

KAMLAND aims at detecting the $\overline{\nu}_e$ produced by five nuclear reactors located at distances between 150 and 210 km from the detector and producing a total thermal power of 127 GW. When all reactors run at full power, the event rate is expected to be $\sim$ 2 d^{-1} with a signal-to-noise ratio of 10. The background is measured by observing the variation of the event rate with the reactor power.

Because of its large distance from the reactors, KAMLAND is sensitive to $\Delta m^2 > 7 \times 10^{-6}$ eV^2 and $\sin^2 2\theta > 0.1$, a region which includes the large mixing angle, large Δm^2 MSW solution of the solar neutrino problem [9]. The anticipated exclusion region after three years of data taking in the absence of neutrino oscillations is shown in Fig. 4.

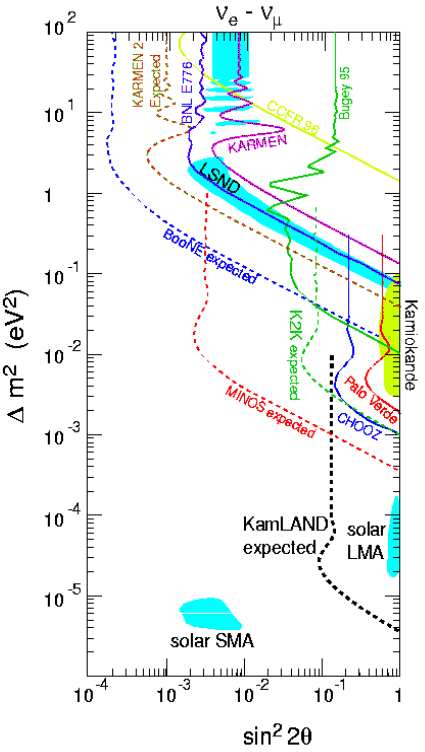

Figure 4: Region of $\overline{\nu}_e - \overline{\nu}_x$ oscillation parameters excluded at the 90% confidence level if no oscillation signal is detected by KAMLAND after three years of data taking. Also shown are regions of oscillation parameters allowed or excluded by other experiments. The solar large mixing angle (LMA) and small mixing angle (SMA) MSW solutions are also visible.

4 Searches for $\nu_\mu - \nu_e$ oscillations at accelerators

The Liquid Scintillator Neutrino Detector (LSND) [10] and the KArlsruhe-Rutherford Medium Energy Neutrino (KARMEN) experiment [11] use neutrinos produced in the beam stop of a proton accelerator. LSND has finished data taking at the Los Alamos Neutron Science Center (LANSCE) at the end of 1998, while KARMEN is still running at the ISIS neutron spallation facility of the Rutherford-Appleton Laboratory.

In these experiments, neutrinos are produced by the following decay processes:

(i) $\pi^+ \to \mu^+ \nu_\mu$ (in flight or at rest);

(ii) $\mu^+ \to \overline{\nu}_\mu e^+ \nu_e$ (at rest);

(iii) $\pi^- \to \mu^- \overline{\nu}_\mu$ (in flight);

(iv) $\mu^- \to \nu_\mu e^- \overline{\nu}_e$ (at rest).

The $\overline{\nu}_e$ yield is very small (of the order of 4×10^{-4} with respect to $\overline{\nu}_\mu$) because π^- decaying in flight are a few % of all produced π^- and only a small fraction of μ^- stopping in heavy materials decays to $\nu_\mu e^- \overline{\nu}_e$ (π^- at rest are immediately captures by nuclei; most μ^- stopping in high-Z materials undergo the capture process $\mu^- p \to \nu_\mu n$).

Table 2 lists the main parameters of the two experiments. For the $\overline{\nu}_\mu - \overline{\nu}_e$ oscillation search, the $\overline{\nu}_e$ is detected by reaction (3). The delayed neutron signal results from the 2.2 MeV γ-ray from the reaction $np \to d\gamma$ and also, for KARMEN, the 8 MeV line from γ-rays emitted by neutron capture in Gadolinium, which is contained in thin layers of Gd_2O_3 placed between adjacent cells.

While the LANSCE beam is ejected in $\sim 500 \mu$s long spills 8.3 ms apart, the ISIS beam is pulsed with a time structure consisting of two 100 ns long pulses separated by 320 ns (this sequence has a repetition rate of 50 Hz). Thus, it is possible to separate neutrinos from muon and pion decay from their different time distributions with respect to the beam pulse.

Table 3 lists preliminary results from LSND [12] and KARMEN [13], obtained after requiring space and time correlation between the prompt and delayed signal, as expected from $\overline{\nu}_e p \to e^+ n$ (and for KARMEN, requiring also the time correlation between the e^+ signal and the beam pulse). The LSND result gives evidence for an excess of $\overline{\nu}_e$ events with a statistical significance of ~ 4.5 standard deviations.

Figure 5 shows the preliminary e^+ energy distribution of the 70 events observed by LSND, together with the distributions expected from backgrounds and from $\overline{\nu}_\mu - \overline{\nu}_e$ oscillations for two different Δm^2 values. The region of oscillation parameters describing the LSND result is shown in Fig. 6, together with the region excluded by the Bugey reactor experiment [14] and by the present KARMEN result. This figure

	LSND	KARMEN
Proton Kin. Energy	800 MeV	800 MeV
Proton beam current	1000 μA	200 μA
Detector	Single cylindrical tank; 1220 PMT's; collection of both scintillation and Čerenkov light.	512 cells filled with liquid scintillator; cell dim. 18 × 18 × 350 cm
Detector mass	167 tons	56 tons
Event localization	timing	cell size
Distance from ν source	29 m	17 m
Angle between ν direction and proton beam	17°	90°
Data taking period	1993–98	Feb. 97–Feb. 99
Protons on target	1.8×10^{23}	2.9×10^{22}

Table 2: Parameters of the LSND and KARMEN experiments.

shows that, if the LSND result is correct, the only allowed region of $\overline{\nu_\mu} - \overline{\nu}_e$ oscillation parameters is a narrow strip with Δm^2 between 0.2 and 2 eV^2 and $\sin^2 2\theta$ between 0.002 and 0.04.

During the first three years of LSND data taking, the target area of the LANSCE accelerator consisted of a 30 cm long water target located ~ 1 m upstream of the beam stop. This configuration enhanced the probability of pion decay in flight, allowing LSND to search for $\nu_\mu - \nu_e$ oscillations using ν_μ with energy above 60 MeV. In this case, one expects to observe an excess of events from the reaction

$$\nu_e + C^{12} \rightarrow e^- + X$$

	LSND [12]	KARMEN [13]
e^+ energy interval	20–60 MeV	16–50 MeV
Observed events	70	8
Cosmic ray background	17.7 ± 1.0	1.9 ± 0.1
Total background	30.5 ± 2.7	7.82 ± 0.46
$\overline{\nu}_e$ signal events	39.5 ± 8.8	< 3.4 (90% C.L)
$\overline{\nu_\mu} - \overline{\nu}_e$ oscillation probability	$(3.3 \pm 0.9 \pm 0.5) \times 10^{-3}$	$< 1.03 \times 10^{-3}$ (90% C.L.)

Table 3: Preliminary results from LSND and KARMEN.

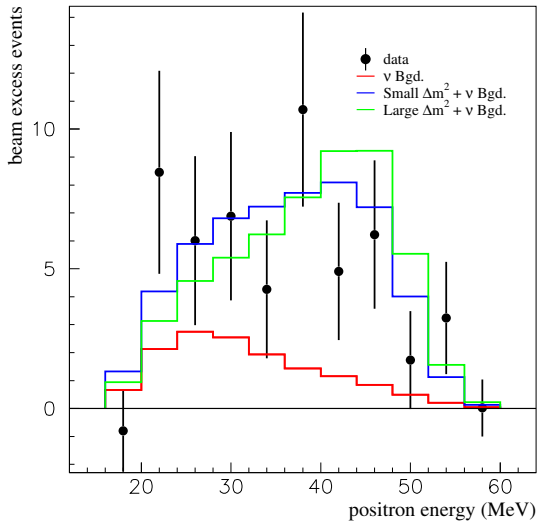

Figure 5: Preliminary e^+ energy distribution of the 70 events observed by LSND. Also shown are the distributions expected from backgrounds (histogram with error bars) and the expectations from $\overline{\nu}_\mu - \overline{\nu}_e$ oscillations for two different Δm^2 values.

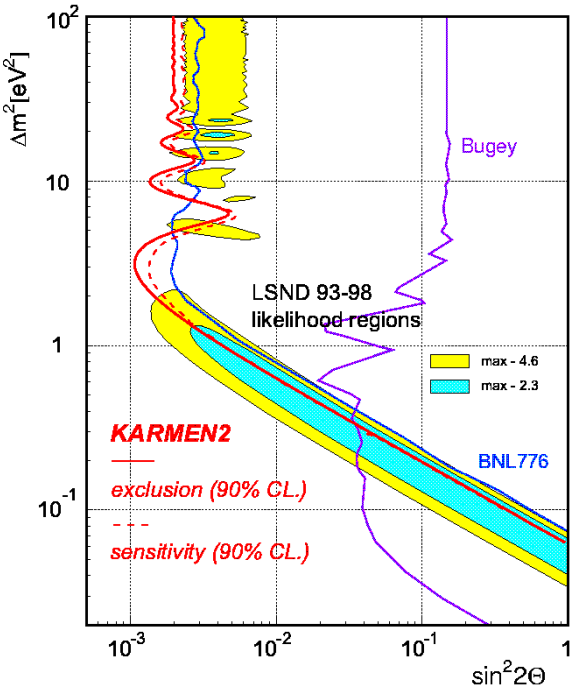

Figure 6: Region of $\overline{\nu}_\mu - \overline{\nu}_e$ oscillation parameters allowed by the preliminary LSND results [12]. Also shown are the boundaries of the regions excluded by the Bugey reactor experiment [14] and by the recent KARMEN result [13].

above the expected backgrounds. This reaction has only one signature (a prompt signal) but the higher energy, the longer track and the directionality of Čerenkov light help improving electron identification and measuring its direction.

In this search [15], LSND has observed 40 events to be compared with 12.3 ± 0.9 events from cosmic ray background and 9.6 ± 1.9 events from machine-related (neutrino-induced) processes. The excess of events (18.1 ± 6.6 events) corresponds to a $\nu_\mu - \nu_e$ oscillation probability of $(2.6 \pm 1.0) \times 10^{-3}$, consistent with the value found from the study of the $\overline{\nu}_e p \to e^+ n$ reaction below 60 MeV.

In view of the importance of the LSND result, it is useful to review other measurements of conventional neutrino processes in the LSND experiment and to compare them with theoretical predictions [12]. Such a comparison is presented in Table 4. There is general agreement between the measured and predicted values, except for the last reaction in Table 4. However, in this case, the experimental value for the cross-section is lower than the predicted one and the theoretical calculation is difficult because of nuclear effects.

Reaction	σ_{theory} (cm^2)	LSND measurement	
		Events above background	σ_{meas} (cm^2)
$\nu_e + C^{12} \to e^- + N^{12}$	9.3×10^{-42}	515	$(9.1 \pm 0.4 \pm 0.9) \times 10^{-42}$
$\nu_e + C^{12} \to e^- + (N^{12})^*$	6.3×10^{-42}	660	$(5.7 \pm 0.6 \pm 0.6) \times 10^{-42}$
$\nu_\mu + C^{12} \to \mu^- + N^{12}$	6.4×10^{-41}	57	$(6.6 \pm 1.0 \pm 1.0) \times 10^{-41}$
$\nu_\mu + C^{12} \to \mu^- + (N^{12})^*$	20.5×10^{-40}	1738	$(11.2 \pm 0.3 \pm 1.8) \times 10^{-40}$

Table 4: Cross-sections for conventional neutrino processes: theoretical predictions and LSND measurements [12].

4.1 Future searches for $\nu_\mu - \nu_e$ oscillations at accelerators

The KARMEN experiment will finish data taking in the year 2001. By then, its sensitivity to $\overline{\nu}_\mu - \overline{\nu}_e$ oscillations will have improved by a factor of 1.7 with respect to the present value. However, in case of a negative result the exclusion region will not fully contain the region allowed by LSND. A new search for $\nu_\mu - \nu_e$ (or $\overline{\nu}_\mu - \overline{\nu}_e$) oscillations is needed, therefore, to unambiguously confirm or refute the LSND signal.

The Mini-BooNE experiment [16] is a first phase of a new, high sensitivity search for $\nu_\mu - \nu_e$ oscillations (BooNE is the acronym for Booster Neutrino Experiment). Neutrinos are produced using an 8 GeV, high intensity proton beam from the Fermilab Booster Synchrotron. The beam consists mainly of ν_μ from π^+ decay with a small contamination ($\sim 0.3\%$) of ν_e and a broad energy distribution from 0.3 to 2 GeV.

The Mini-BooNE detector will be installed at a distance of 500 m from the neutrino source. It consists of a 6 m radius spherical tank filled with mineral oil. Čerenkov light produced in the oil is collected by ~ 1500 photomultiplier tubes located on the surface of the sphere. The detector is surrounded by anticoincidence counters and will use the different pattern of Čerenkov light expected for muons, electrons, and π^0 to identify these particles. For a fiducial mass of 445 tons, Mini-BooNE expects to detect $\sim 5 \times 10^5$ $\nu_\mu\, C^{12} \to \mu^- X$ events and ~ 1700 $\nu_e C^{12} \to e^- X$ events in one year. A $\nu_\mu - \nu_e$ oscillation with the parameters required to describe the LSND signal would result in an excess of ~ 1500 $\nu_e\, C^{12} \to e^- X$ events.

If no oscillation signal is observed, Mini-BooNE will exclude the region of oscillation parameters shown in Fig. 7. However, if a signal is observed, it should be possible to measure precisely the oscillation parameters by using a second detector at a different distance.

Mini-BooNE will begin taking data in the year 2002.

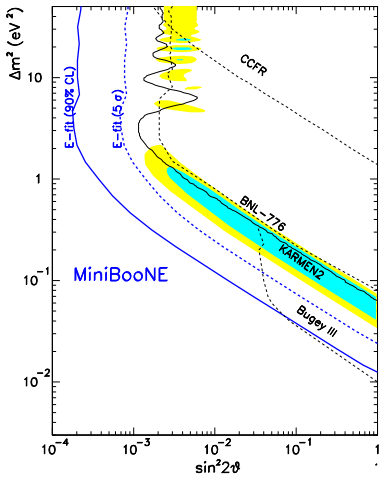

Figure 7: Region of $\nu_\mu - \nu_e$ oscillation parameters excluded by Mini-BooNE if no signal is observed after one year of data taking.

4.2 Searches for $\nu_\mu - \nu_\tau$ oscillations

Two experiments searching for $\nu_\mu - \nu_\tau$ oscillations have recently completed data taking at CERN. They both used the wide-band neutrino beam from the CERN 450 GeV proton synchrotron (SPS). The method adopted by both experiments consists in detecting τ^- production with a sensitivity corresponding to a ν_τ/ν_μ ratio much larger than the value expected from conventional ν_τ sources in the beam. (The main ν_τ production process is D_s production by the primary protons, followed by the de-

cay $D_s \to \tau\nu_\tau$.) The observation of τ^- could only result, therefore, from $\nu_\mu - \nu_\tau$ oscillations.

The two experiments, CHORUS and NOMAD, are installed one behind the other at a distance of $\sim$ 820 m from the proton target. The distance between the proton target and the end of the decay tunnel is 414 m. Table 5 lists the mean neutrino energies and relative abundances. The ν_τ 'natural' abundance is estimated to be $\sim 5 \times 10^{-6}$ [17].

	Flux		Charged-current interactions	
ν type	$< E_\nu >$ GeV	Relative abundance	$< E_\nu >$ GeV	Relative abundance
ν_μ	23.5	1.00	42.6	1.00
$\overline{\nu}_\mu$	19.2	0.061	41.0	0.0249
ν_e	37.1	0.0094	56.7	0.0148
$\overline{\nu}_e$	31.3	0.0024	53.6	0.0016
ν_τ	~ 35	$\sim 5 \times 10^{-6}$		

Table 5: Mean energies and relative abundances for ν fluxes and CC interactions at the NOMAD detector. The integrated ν_μ flux is 1.11×10^{-2} ν_μ per proton on target.

CHORUS (CERN Hybrid Oscillation Research apparatUS) aims at detecting the decay of the short-lived τ lepton in nuclear emulsion. This technique provides a space resolution of $\sim$ 1 μm, well matched to the average τ^- decay length of 1 mm.

The apparatus [18] consists of an emulsion target with a total mass of $\sim$ 770 kg, followed by an electronic tracking detector made of scintillating fibres, an aircore hexagonal magnet, electromagnetic and hadronic calorimeters and a muon spectrometer consisting of magnetized iron toroids interleaved with drift chambers. Neutrino events with a μ^- or a negatively charged hadron are selected and the tracks are followed back to the exit point from the emulsion target. The method is illustrated in Fig. 8. It relies on special emulsion sheets mounted between the target and the fibre tracker (these sheets are replaced every few weeks during the run). With the reconstruction accuracy of the fibre tracker, the track position on the special sheet is predicted within an area of 360 μm $\times$ 360 μm. In this area, because of the short exposure time, one finds, an average, 5 muon tracks which are rejected by angular measurement. The search is then continued in an area of 20 μm $\times$ 20 μm into the emulsion target, with negligible background despite the long exposure time of the target (2 years).

Events in which the neutrino interaction point is found in the emulsion target are analyzed to search for τ^- decay, which is identified by the presence of a change in direction (kink) of a negatively charged track, as expected from one-prong decays. No other charged leptons must be observed at the primary vertex and the transverse

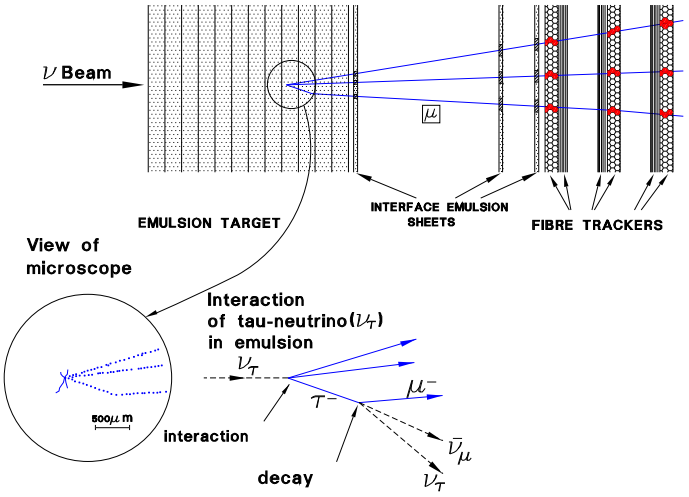

Figure 8: Expected configuration of a typical ν_τ charged-current interaction in the CHORUS emulsion. In this example the τ^- decays to $\mu^-\nu_\tau\overline{\nu}_\mu$.

momentum (p_T) of the selected particle with respect to the τ candidate direction is required to be larger than 0.25 GeV (to eliminate strange particle decays). Negative tracks with impact parameters larger than $\sim$ 8 μm are also considered as possible secondary particles from τ^- decay.

Negative muons with momentum $p < 30$ GeV or negative hadrons with $1 < p < 20$ GeV are considered as possible τ^- decay products. If observed, the kink is required to be within 3.95 mm from the interaction point for muon tracks, and 2.37 mm for hadron tracks. The emulsion scanning procedure to locate the interaction point and to reject events incompatible with τ^- decays is fully automatic. The remaining events undergo a computer assisted eye scan to confirm the presence of a τ decay.

CHORUS took data between May 1994 and the end of 1997. Table 6 summarizes the present status of the analysis [19]. No τ^- candidate has been observed yet.

	One-muon events	Muonless events
Expected number of events	458.6×10^3	116×10^3
Fraction scanned so far	54%	47%
Events with identified ν interaction	126.2×10^3	19.4×10^3
N_τ for $< P_{\mu\tau} > = 1$	4876	1137

Table 6: Status of the CHORUS analysis [19]

The dominant background in the one-muon channel is the production of charmed particles from $\overline{\nu}_\mu$ interactions

$$\overline{\nu}_\mu \; N \rightarrow \mu^+ D^- X$$

followed by the decay $D^- \rightarrow \mu^-$ + neutral particles. These events are dangerous only if the μ^+ is not identified. Their contribution to the data sample analyzed so far is 0.24 ± 0.05 events. In the muonless channel, the background from charm production amounts to 0.075 ± 0.015 events. A more serious background is the interaction of negative hadrons with nuclei producing only one outgoing negatively charged particle with no evidence for nuclear break-up (these interactions are called 'white kinks'). The rate of such events, of the order of one event, is affected by a large uncertainty.

The expected numbers of events, N_τ, for an oscillation probability $P_{\mu\tau} = 1$, are given in the last row of Table 6. The 90% confidence upper limit on $P_{\mu\tau}$ is

$$P_{\mu\tau} < 4.0 \times 10^{-4} \; .$$

The region of oscillation parameters excluded by this result under the assumption of two-neutrino mixing is shown in Fig. 9 together with the results from previous experiments [20]. A more stringent limit, $P_{\mu\tau} < 2.6 \times 10^{-4}$, would be obtained [21] using the method recently proposed by Feldman and Cousins [22].

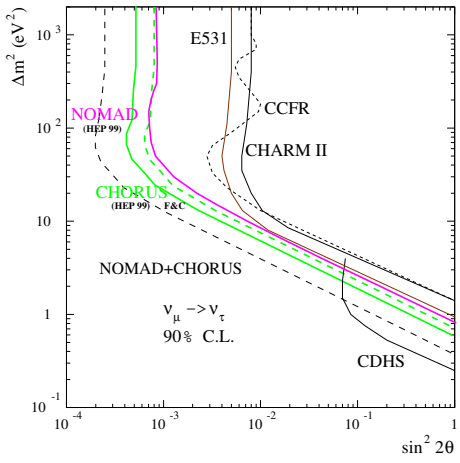

Figure 9: The $\Delta m^2 - \sin^2(2\theta)$ plane for $\nu_\mu - \nu_\tau$ oscillation. The regions excluded by CHORUS and NOMAD, and by their combined results [21], are shown together with the results of previous experiments [20]. Full lines: CHORUS (for two different statistical methods); dashed lines: NOMAD and combined result.

CHORUS is expected to reach the upper limit $P_{\mu\tau} < 10^{-4}$ if no event is found after the completion of the analysis.

NOMAD (Neutrino Oscillation MAgnetic Detector) is designed to search for $\nu_\mu - \nu_\tau$ oscillations by observing τ^- production using kinematical criteria [23], which require a precise measurement of secondary particle momenta. The main detector components are [24] (see Fig. 10):

- drift chambers (DC) used to reconstruct charged particle tracks and also acting as the neutrino target (fiducial mass $\sim$ 2.7 tons, average density 0.1 g/cm^3, radiation length $\sim$ 5 m);
- nine independent transition radiation detectors (TRD) for electron identification, interleaved with additional drift chambers;
- an electromagnetic calorimeter (ECAL) located behind a 'preshower' detector (PRS);
- a hadronic calorimeter (HCAL);
- large-area muon chambers.

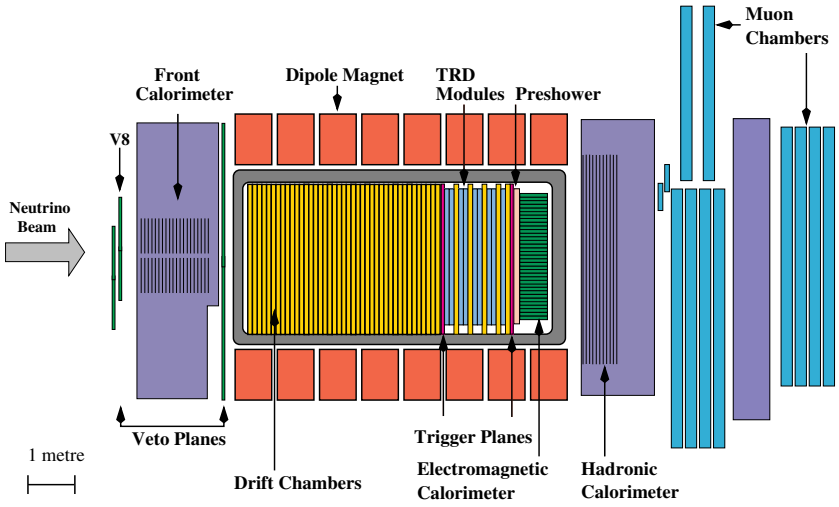

Figure 10: Side view of the NOMAD detector.

DC, TRD, and ECAL are located inside a uniform magnetic field of 0.4 T perpendicular to the beam direction.

The NOMAD experiment aims at detecting τ^- production by observing both leptonic and hadronic decay modes of the τ^-. The decay $\tau^- \to \nu_\tau e^- \overline{\nu}_e$ is particularly attractive because the main background results from ν_e charged-current interactions which are only $\sim$ 1.5% of the total number of neutrino interactions in the target fiducial volume and have an energy spectrum quite different from that expected from

$\nu_\mu - \nu_\tau$ oscillations (see Table 6). The selection of this decay relies on the presence of an isolated electron in the final state and on the correlation among the lepton transverse momentum ($\vec{p}_T^{\,e}$), the total transverse momentum of the hadronic system ($\vec{p}_T^{\,H}$) and the missing transverse momentum ($\vec{p}_T^{\,m}$) (only the momentum components perpendicular to the beam direction can be used because the incident neutrino energy is unknown). In the case of ν_e charged-current events $\vec{p}_T^{\,e}$ is generally opposite to $\vec{p}_T^{\,H}$ and $|\vec{p}_T^{\,m}|$ is small (it should be exactly zero if the momenta of all secondary particles were measured precisely and the target nucleon were at rest). On the contrary, in $\tau^- \to \nu_\tau e^- \overline{\nu}_e$ decays there is a sizeable $|\vec{p}_T^{\,m}|$ associated with the two outgoing neutrinos. Furthermore, in a large fraction of events, $\vec{p}_T^{\,m}$ is at opposite azimuthal angles to $\vec{p}_T^{\,H}$, in contrast with ν_e charged-current interactions for which large values of $|\vec{p}_T^{\,m}|$ result mostly from hadrons escaping detection (in these cases the azimuthal separation between $\vec{p}_T^{\,H}$ and $\vec{p}_T^{\,m}$ is small).

In practice, for most τ^- decay channels, the method to separate the signal from backgrounds uses ratios of likelihood functions. These functions are approximated by products of probability density functions of kinematic variables. These are obtained from large samples of simulated events, after corrections to take into account differences between simulated and real data, as described in Ref. [25].

Table 7 shows a summary of backgrounds and efficiencies for separate analyses of deep-inelastic scattering events (DIS) and low-multiplicity (LM) events reported in Ref. [26] (DIS events are defined by the requirement $p^H > 1.5$ GeV). For all channels, there is good agreement between the observed number of events and the background prediction. The resulting 90% confidence level upper limit using the method of Ref. [22] is [26]

$$P_{\mu\tau} < 4.2 \times 10^{-4} \ ,$$

which corresponds to the exclusion region shown in Fig. 9.

The CHORUS and NOMAD limits can be combined using the method of Ref. [22]. The combined limit is [21]

$$P_{\mu\tau} < 1.3 \times 10^{-4} \ .$$

The corresponding exclusion region is outlined in Fig. 9.

5 Long baseline experiments at accelerators

Long baseline experiments at accelerators extend the sensitivity of searches for $\nu_\mu - \nu_x$ oscillations to Δm^2 as low as 10^{-3} eV^2 using ν_μ beams of well known properties which can be monitored and varied if needed. The main goal of these experiments is to verify that the atmospheric neutrino results [6] are indeed associated with oscillations, to establish the nature of the oscillation and to measure its parameters. As discussed in Ref. [6], the most plausible interpretation of the atmospheric neutrino results is the occurrence of $\nu_\mu - \nu_\tau$ oscillations with $\Delta m^2 \approx 3.5 \times 10^{-3}$ eV^2 and full mixing. A

Analysis	N_τ	Estimated background	Observed number of events
$\tau^- \to e^-$ DIS	4110	$5.3^{+0.6}_{-0.4}$	5
$\tau^- \to h^-(n\pi^0)$ DIS	2232	6.8 ± 2.1	6
$\tau^- \to \rho^-$ DIS	2547	$7.3^{+2.2}_{-1.2}$	8
$\tau^- \to \pi^-\pi^-\pi^+$ DIS	1180	6.5 ± 1.1	5
$\tau^- \to e^-$ LM	859	5.4 ± 0.9	6
$\tau^- \to h^-$ LM	357	6.7 ± 3.0	5
$\tau^- \to \rho^-$LM	457	5.2 ± 2.4	7
$\tau^- \to \pi^-\pi^-\pi^+$ LM	108	$0.4^{+0.6}_{-0.4}$	0

Table 7: Summary of NOMAD results [26]. N_τ is the number of expected τ^- events for $P_{\mu\tau} = 1$

$\nu_\mu - \nu_s$ oscillation, where ν_s is a new, 'sterile' neutrino, is also possible, though less favored.

Table 8 shows a list of parameters for the three existing projects.

Project	Accelerator	Location of far detector	Distance (Km)	$< E_\nu >$ GeV	Status
K2K	KEK 12 GeV proton synchrotron	Kamioka mine	250	1.4	Start April 1999
NuMI	Fermilab 120 GeV Main Injector (MI)	Soudan mine	730	16 or lower	Start 2002
CNGS	CERN 450 GeV SPS	Gran Sasso Lab	732	30 or lower	not yet approved

Table 8: Long baseline projects

5.1 K2K

The K2K project [27] uses neutrinos from the decay of π and K mesons produced by the KEK 12 GeV proton synchrotron and aimed at the SuperKamiokande detector at a distance of 250 km. The beam consists mainly of ν_μ, with an average energy of 1.4 GeV. The $\overline{\nu}_\mu$ and ν_e contaminations are 4% and 1%, respectively. The energy is below threshold for τ^- production ($E_\nu \approx 3.5$ GeV), so no search for τ^- appearance is possible.

The expected distortion of the ν_μ flux at 250 km for a ν_μ oscillation with $\Delta m^2 =$

3.5×10^{-3} eV^2 can be detected by comparing the energy distribution of beam-associated muon-like events in SuperKamiokande with the distribution measured in a similar, 1 Kton water detector located at 300 m from the neutrino source on the KEK site where no oscillation effects are expected.

The near detector includes a system of scintillating fibres in water, a lead glass calorimeter and a muon range telescope to monitor and measure precisely the ν_μ, $\overline{\nu}_\mu$, and ν_e energy spectra and space distributions. The 1 Kton water detector will also measure the cross-section for π^0 production in neutral-current interactions. The knowledge of this quantity helps understanding if the disappearance of atmospheric ν_μ's is the result of oscillations to an active or to a sterile neutrino.

Expected event rates for a run of 10^{20} protons on target (3 years, corresponding to an effective data taking time of 12 months) are given in Table 9. Figure 11 shows the region of $\nu_\mu - \nu_x$ oscillation parameters which will be excluded if no significant difference is observed between the near and far detector.

	Near detector		
	Fine-grained	1 Kton water	Super-K
Fiducial mass	4 tons	21 tons	22,500 tons
ν_μ CC events	126,700	408,000	345
ν_μ NC events	44,900	144,000	120
π°-like events	9,200	29,500	25
ν_e CC events	1,250	4,000	4

Table 9: Event rates in the K2K experiment for 10^{20} protons on target.

The K2K experiment has taken the first data between March and June 1999. Interactions of beam neutrinos in the Super-Kamiokande detector are identified by their timing because the beam spill is only 1 μs wide. Clocks at the near and far detector are synchronized with an accuracy of 100 ns using time signals provided by the Global Positioning System (GPS). During this running period four events have occurred in a time window of $\pm 50\mu$s centered on the arrival time of the neutrino beam pulse. These events are all contained in a 1 μs wide bin at $t = 0$, demonstrating their beam origin. Of these, only one event (with two Čerenkov rings) is a neutrino interaction in the fiducial volume of the Super-Kamiokande detector.

The K2K experiment has resumed data taking at the end of October 1999.

5.2 NuMI and the MINOS experiment

The NuMI project uses neutrinos from the decay of π and K mesons produced by the new Fermilab Main Injector (MI), a 120 GeV proton synchrotron capable of

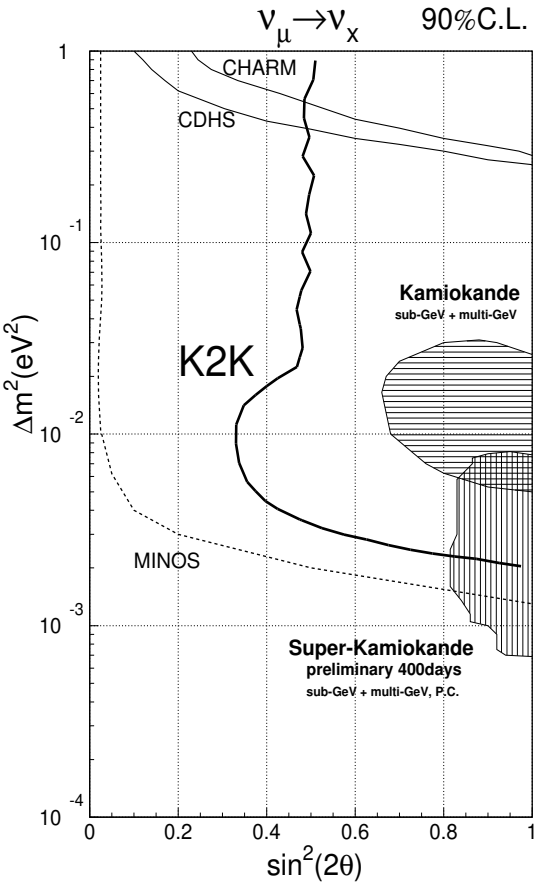

Figure 11: Region of $\nu_\mu - \nu_\tau$ or $\nu_\mu - \nu_s$ oscillation parameters excluded at the 90% confidence level if no oscillation signal is detected by the K2K experiment after three years of data taking.

accelerating 5×10^{13} protons with a cycle time of 1.9 s. The expected number of protons on target is 3.6×10^{20}/y. The decay pipe is 675 m long.

The neutrino beam will be aimed at the Soudan mine in Minnesota at a distance of 730 km from the proton target. The beam will consist primarily of ν_μ, with 0.6% ν_e. Three different neutrino beams have been designed, with average energies of ~ 3, 8, and 16 GeV corresponding to different tunes and locations of the focusing elements. For the high energy beam, the expected number of events is ~ 3000/y for a detector mass of 1000 tons.

For an oscillation with $\Delta m^2 = 3.5 \times 10^{-3}$ eV^2, the ν_μ flux at 730 km is maximally suppressed at neutrino energies of 2 GeV. Such a distortion can be best detected using the lowest energy beam.

The MINOS experiment [28] will use two detectors, one (the 'near detector') located at Fermilab, the other (the 'far detector') located in a new underground hall

to be built at the Soudan site at a depth of 713 m (2090 m of water equivalent). Both detectors are iron-scintillator sandwich calorimeters with a toroidal magnetic field in the iron plates.

The far detector (Fig. 12) has a total mass of 5400 tons and a fiducial mass of 3300 tons. It consists of magnetized octagonal iron plates, 2.54 cm thick, interleaved with active planes of 4 cm wide, 8 m long scintillator strips providing both calorimetric and tracking information. The near detector has a total mass of 920 tons and a fiducial mass of 100 tons. It will be installed 250 m downstream from the end of the decay pipe.

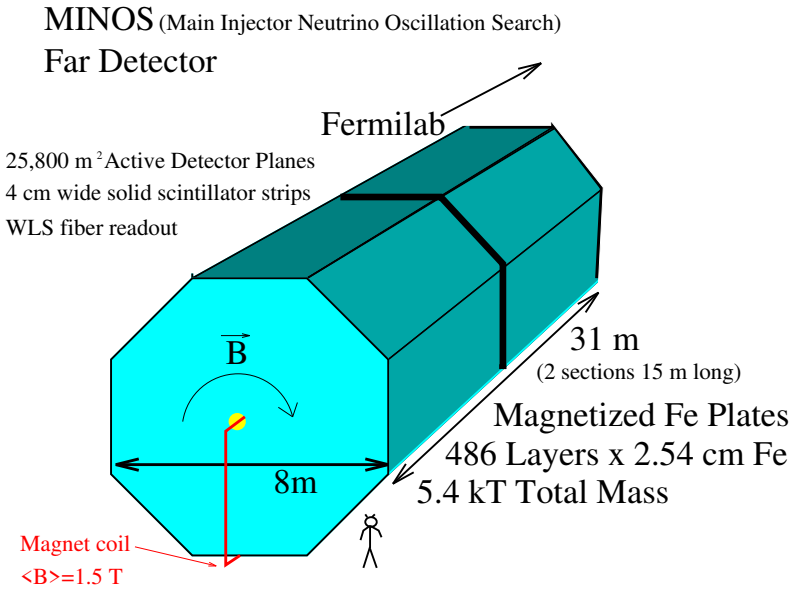

Figure 12: Sketch of the MINOS detector at the far location.

The comparison of ν_μ charged-current event rate and energy distribution in the two detectors will be sensitive to oscillations which can be detected with a statistical significance of at least four standard deviations over the full parameter space currently suggested by the atmospheric neutrino results (see Fig. 13). The oscillation parameters will be measured precisely over most of this region.

The measurement of the ratio between neutral- and charged-current event rate (NC/CC) is very important because it will be used to discriminate between $\nu_\mu - \nu_\tau$ and $\nu_\mu - \nu_s$ oscillations. In the former case, NC/CC is larger in the far detector, while for $\nu_\mu - \nu_s$ oscillations, it has the same value in the near and far detector.

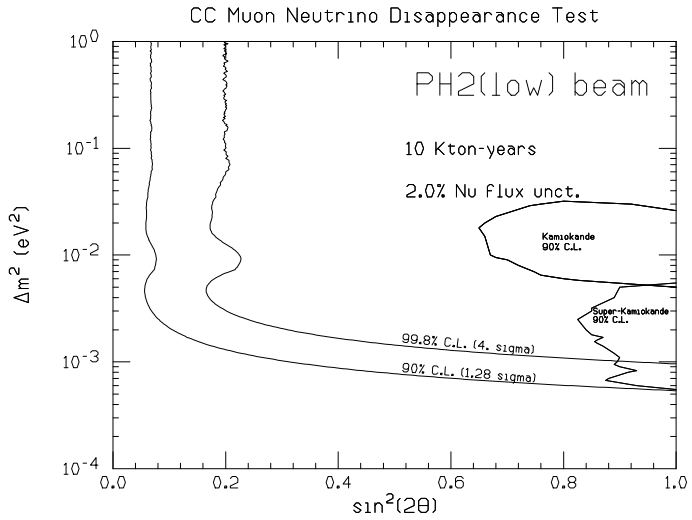

Figure 13: Excluded region (90% confidence) and 4σ discovery region for a 10 kton $\times$ y exposure of the MINOS experiment from a comparison of the ν_μ CC event spectra in the far and near detector.

The MINOS experiment should begin data taking at the end of the year 2002.

5.3 The CNGS project

The CNGS project (CERN Neutrinos to Gran Sasso) has not yet been approved. It consists in aiming a neutrino beam from the CERN 450 GeV SPS to the Gran Sasso National Laboratory in Italy, at a distance of 732 km. The three existing underground halls at Gran Sasso, under ~ 4000 m of water equivalent, are already oriented towards CERN. ICARUS [29], a 600 ton detector suitable for oscillation searches, will start operation in the year 2001 to search for proton decay and to study atmospheric and solar neutrinos.

If approved before the end of 1999, the CNGS beam will be operational in the year 2005. It will be used for ν_τ appearance experiments, for which a detector in a 'near' location should not be necessary. The rate of ν_τ charged-current interactions from $\nu_\mu - \nu_\tau$ oscillations is given by

$$N_\tau = A \int \phi_{\nu_\mu}(E)\ P_{\mu\tau}(E)\ \sigma_\tau(E)\ dE \tag{5}$$

where A is a normalization constant proportional to the detector mass, $\phi_{\nu_\mu}(E)$ is the ν_μ energy spectrum at the detector, $P_{\mu\tau}(E)$ is the $\nu_\mu - \nu_\tau$ oscillation probability and $\sigma_\tau\ (E)$ is the cross-section for ν_τ charged-current interactions. The integration lower limit is set by the energy threshold for τ^- production, 3.5 GeV.

Under the assumption of two-neutrino mixing, $P_{\mu\tau}(E)$ is given by Eq. (2). For a large fraction of the Δm^2 interval suggested by the atmospheric neutrino results, the condition $1.27\ \Delta m^2\ L/E < 1$ holds for $L = 732$ km and $E > 3.5$ GeV. In this case, Eq. (5) can be approximated as

$$N_\tau = 1.61\ A\ \sin^2(2\theta)\ (\Delta m^2)^2\ L^2\ \int\ \phi_{\nu_\mu}(E)\sigma_\tau(E)\frac{dE}{E^2}\ . \qquad (6)$$

In this approximation, N_τ varies as $(\Delta m^2)^2$ and the neutrino beam must be designed with the goal of maximizing the integral of Eq. (6) which does not depend on Δm^2. A preliminary beam design, based on a 1000 m long decay tunnel, is described in Ref. [30]. The design has been improved [31] to optimize the τ^- production rate. The ν_μ mean energy is 17 GeV and the rate of ν_μ charged-current interactions is 2448/y for a detector with a mass of 1000 tons (this value corresponds to 4.5×10^{19} protons on target, which is a realistic figure for a one-year run after the shut-down of LEP).

The rates of other neutrino events relative to ν_μ events are 0.007, 0.02, and 0.0007 for ν_e, $\overline{\nu}_\mu$, and $\overline{\nu}_e$, respectively. Table 10 lists the expected yearly rates of τ^- events [31] for three different Δm^2 values.

Δm^2 (eV^2)	N_τ
10^{-3}	2.48
3×10^{-3}	21.7
5×10^{-3}	58.5

Table 10: Yearly rate of τ^- events vs Δm^2 for a 1000 ton detector [31] (1 year = 4.5×10^{19} protons on target).

ICARUS [29] is a new detector concept based on a liquid Argon Time Projection Chamber (TPC) which allows three-dimensional reconstruction of events with spatial resolution of the order of 1 mm. A 600 ton ICARUS module is presently being constructed. The cryostat cold volume (534 m^3) is 19.6 m long and 4.2 m high. Three additional modules will be built if the operation of the first module is successful.

ICARUS will search for τ appearance using kinematical criteria similar to those used in the NOMAD experiment (see Section 4.2). However, for the $\tau^- \to e^-$ decay channel, a background rejection power in excess of 10^4 was needed in NOMAD, while in ICARUS, a rejection power of $\sim\ 10^2$ is sufficient because of the much smaller number of events. This allows looser selection criteria and the detection efficiency for $\tau^- \to e^-$ events becomes $\sim 50\%$. With four modules, one expects $\sim\ 10\ \tau^-$ events/y for a $\nu_\mu - \nu_\tau$ oscillation with $\Delta m^2 = 5 \times 10^{-3}$ eV^2 and full mixing, to be compared with a background of 0.25 events.

The τ identification for other τ decay channels is presently under study. Because the τ^- production rate at low Δm^2 is proportional to $(\Delta m^2)^2$, a detector consisting of four ICARUS modules should be sensitive to oscillations with $\Delta m^2 \geq 2 \times 10^{-3}$ eV^2 after a running time of four years.

Very recently, a new detector (ICANOE) with a total active mass of 9,300 tons has been proposed [32]. This detector consists of several ICARUS modules interleaved with conventional calorimeters made of magnetized iron.

Another interesting detector concept for a ν_τ appearance search is OPERA [33]. The detection of one-prong τ decays is performed by measuring the τ^- decay kink in space, as determined by two track segments measured with very high precision in nuclear emulsion.

Figure 14 illustrates the OPERA concept. The main component of the target are 1 mm thick Pb plates where most neutrinos interact. One-prong τ decays occurring in the 3 mm gap between the emulsion detectors ES1, ES2 are expected to result in observable kinks. ES1 and ES2 consist of two 50 μm thick emulsion layers glued to a 100 μm plastic foil. The 3 mm gap between ES1 and ES2 is filled with a very low density spacer to which ES1 and ES2 are glued to ensure that their relative positions are stable and precisely known.

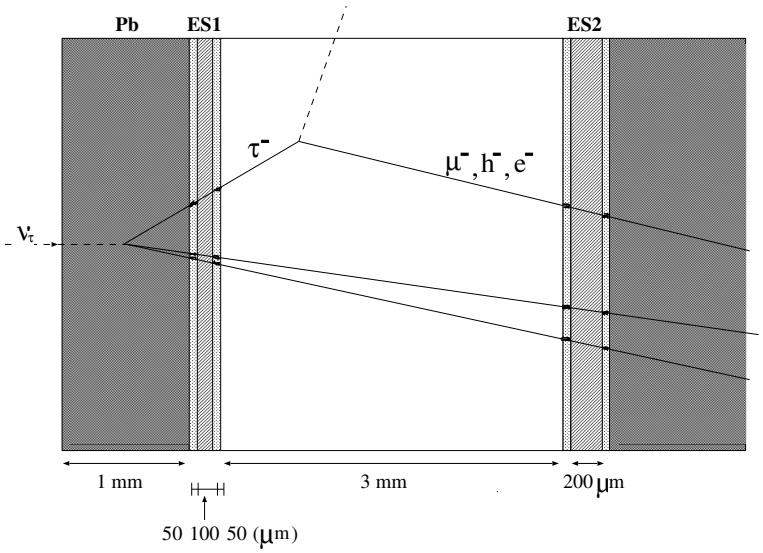

Figure 14: Schematic structure of the OPERA target.

The global τ^- detection efficiency is estimated to vary between 0.29 at low Δm^2 and 0.33 at $\Delta m^2 \approx 10^{-2}$ eV^2. For a run of one year (4.5×10^{19} protons on target) the background is expected to be 0.4 events, mostly from charm production and decay in events in which the primary μ^- was not identified. The number of expected τ^- events for full mixing is listed in Table 11 for different Δm^2 values.

Δm^2 (eV^2)	Detected N^-/y
1.0×10^{-3}	0.5
3×10^{-3}	4.5
5.0×10^{-3}	12.0

Table 11: Number of detected τ^- in OPERA per 4.5×10^{19} protons on target (1 year) (from Ref. [33])

6 Searches for new particles using neutrino beams

The NuTeV (E–815) experiment at Fermilab has searched for a hypothetical Neutral Heavy Lepton, L_μ, which mixes with ν_μ. If such a particle exists, it is produced in meson decays such as $K^+ \to \mu^+ L_\mu$, $D^+ \to \mu^+ L_\mu$ or $D^- \to \mu^- \overline{L}_\mu$. It would then be present in the high-energy neutrino beam from the Tevatron.

L_μ is expected to decay to $\mu^-\mu^+\nu_\mu$, $\mu^- e^+ \nu_e$, $\mu^-\pi^+$, or $\mu^-\rho^+$. In the NuTeV experiment, these decays would result in two-track events with a μ^- and a positive track originating in a 34 m long region in front of the detector. Backgrounds from ordinary neutrino interactions in this region are reduced by the use of Helium bags.

No event consistent with L_μ decay has been observed [34]. Figure 15 shows the 90% confidence level upper limit on the mixing parameter U^2 as a function of the L_μ mass.

7 Conclusions

Neutrino experiments at reactors and accelerators have provided a wealth of physics results and will continue to do so in the future. Over the next decade, these experiments will focus on oscillation studies. They will verify that the atmospheric neutrino results are indeed associated with oscillations and will provide more precise measurements of the oscillation parameters. They will also verify the large mixing angle MSW solution of the solar neutrino problem and provide information on the existence (or non-existence) of the fourth, sterile neutrino which is required if three independent Δm^2 values are needed to explain all the observed oscillation signals.

I thank Dario Autiero, Janet Conrad, Guido Drexlin, Klaus Eitel, and Bill Louis for the help provided in preparing this report.

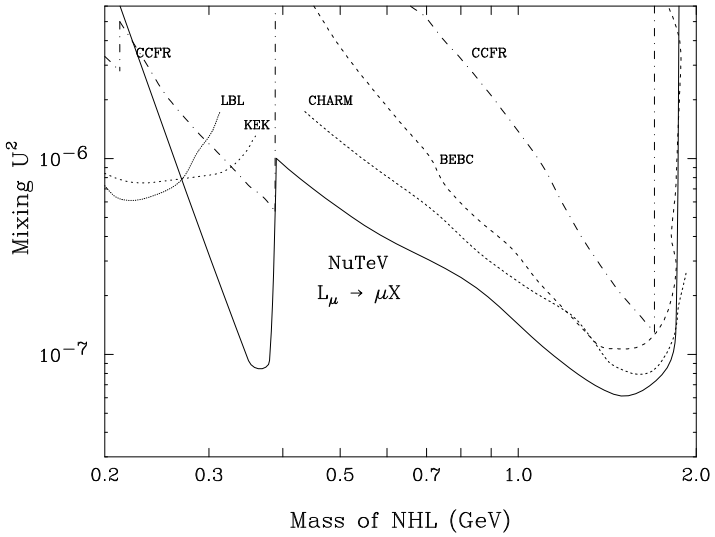

Figure 15: NuTeV 90% confidence level upper limit for U^2, the mixing of Neutral Heavy Leptons (NHL) to ν_μ, as a function of NHL mass (solid line). Also shown are the results from previous experiments.

References

[1] F. Reines and C.L. Cowan, Phys. Rev. **90**, 492 (1953); Phys. Rev. **92**, 830 (1953); C.L. Cowan *et al.*, Science **124**, 103 (1956).

[2] G. Danby *et al.*, Phys. Rev. Lett. **9**, 36 (1962).

[3] Y. Déclais, Nucl. Phys. B (Proc. Suppl.) **70**, 148 (1999).

[4] M. Apollonio *et al.*, Phys. Lett. **B466**, 415 (1999), hep-ex/9907037.

[5] Y. Wang, Recent Results from Palo Verde and Future Prospects, presented at the XXXIV Rencontres de Moriond on Electroweak Interactions and Unified Theories, Les Arcs, France, 13–20 March 1999.

[6] For a review see A. Mann, these proceedings.

[7] Y. Fukuda *et al.*, Phys. Lett. **B335**, 237 (1994).

[8] A. Suzuki, Nucl. Phys. B. (Proc. Suppl.) 77, 171 (1999).

[9] For a review see Y. Suzuki, these proceedings.

[10] C. Athanassopoulos *et al.*, Nucl. Intrum. Methods **A388**, 149 (1997).

[11] B. Zeitnitz, Prog. Part. Nucl. Phys. **32**, 351 (1994).

[12] G. Mills, Results from LSND, presented at the XXXIV Rencontres de Moriond on Electroweak Interactions and Unified Theories, Les Arcs, France, 13–20 March 1999.

[13] T. Jannakos, Latest Results from the Search for $\overline{\nu}_\mu \rightarrow \overline{\nu}_e$ Oscillations with KARMEN2, presented at the XXXIV Rencontres de Moriond on Electroweak Interactions and Unified Theories, Les Arcs, France, 13–20 March 1999; see also http://www-ik1.fzk.de/karmen/karmen.html

[14] B. Achtar *et al.*, Nucl. Phys. **B434**, 503 (1995).

[15] C. Athanassopoulos *et al.*, Phys. Rev. **C58**, 2489 (1998).

[16] E. Church *et al.*, A proposal for an experiment to measure $\nu_\mu - \nu_e$ oscillations and ν_μ disappearance at the Fermilab Booster: BooNE, 7 December 1997 (unpublished).

[17] M.C. Gonzales-Garcia and J.J. Gomez-Cadenas, Phys. Rev. **D55**, 1297 (1997); B. Van de Vijver and P. Zucchelli, Nucl. Instr. and Methods **A385**, 91 (1997).

[18] E. Eskut *et al.*, Nucl. Instr. Methods **A401**, 7 (1997).

[19] The CHORUS Collaboration, hep-ex/9907015.

[20] E531: N. Ushida *et al.*, Phys. Rev. Lett. **57**, 2897 (1986); CHARM-II: M. Gruwé *et al.*, Phys. Lett. **B309**, 463 (1993); CCFR: K.S McFarland *et al.*, Phys. Rev. Lett. **75**, 3993 (1995); CDHS: F. Dydak *et al.*, Phys. Lett. **B134**, 281 (1984).

[21] R. Petti, private communication.

[22] G.J. Feldman and R.D. Cousins, Phys. Rev. **D57**, 3873 (1998).

[23] C. Albright and R. Shrock, Phys. Lett. **B84**, 123 (1979).

[24] J. Altegoer *et al.*, Nucl. Instr. Methods **A404**, 96 (1998).

[25] J. Altegoer *et al.*, Phys. Lett. **B431**, 219 (1998); P. Astier *et al.*, Phys. Lett. **B453**, 169 (1999).

[26] D. Gibin (NOMAD Collaboration), Search for $\nu_\mu - \nu_\tau$ oscillations in the NOMAD experiment, presented at the Int. Europhys. Conf. on High Energy Physics (HEP99), Tampere, Finland, 15–21 July 1999.

[27] K. Nishikawa, Nucl. Phys. B (Proc. Suppl.) 77, 198 (1999).

[28] S. Wojcicki, Nucl. Phys. B (Proc. Suppl.) 77, 182 (1999).

[29] A. Bettini *et al.*, Nucl. Instr. Methods **A332**, 395 (1993); J.P. Revol *et al.*, A search program for explicit neutrino oscillations at long and medium baselines with ICARUS detectors, ICARUS-TM-97/01 (5 March 1997).

[30] G. Acquistapace *et al.*, The CERN neutrino Beam to Gran Sasso, CERN 98–02 (19 May 1998).

[31] A. Ereditato *et al.*, Towards the optimization of the CNGS neutrino beam for $\nu_\mu - \nu_\tau$ appearance experiments, ICARUS-TM/98–13, OPERA 980722–01 (August 10, 1998); J.L. Baldy *et al.*, The CERN Neutrino beam to Gran Sasso (NGS), CERN-SL/99–034 (May 1999).

[32] F. Arneodo *et al.*, ICANOE: Imaging and CAlorimetric Neutrino Oscillation Experiment, INFN/AE–99–17; CERN/SPSC 99–25 (1999).

[33] K. Kodama *et al.*, The OPERA ν_τ appearance experiment in the CERN-Gran Sasso neutrino beam, CERN SPSC 98–25 (October 9, 1999).

[34] A. Vaitaitis *et al.*, hep-ex/9908011.